Robust Magnetic Bearing Control Using Stabilizing Dynamical Compensators

Guang-Ren Duan, *Senior Member, IEEE*, Zhan-Yuan Wu, Chris Bingham, *Member, IEEE*, and David Howe

***Abstract*—This paper considers the robust control of an active radial magnetic bearing system, having a homopolar, external rotor topology, which is used to support an annular fiber composite flywheel rim. A first-order dynamical compensator, which uses only position feedback information, is used for control, its design being based on a linearized one-dimensional second-order model which is treated as an interval system in order to cope with parameter uncertainties. Through robust stability analysis, a parameterization of all first-order robustly stabilizing dynamical compensators for the interval system is initially obtained. Then, by appropriate selection of the free parameters in the robust controller, the H_2 norm of the disturbance-output transfer function is made arbitrarily small over the system parameter intervals, and the H_∞ norm of the input–output transfer function is made arbitrarily close to a lower bound. Simulation and experimental results demonstrate both stability and performance robustness of the developed controller.**

***Index Terms*—Disturbance attenuation, interval systems, magnetic bearing, robust stabilization.**

I. INTRODUCTION

ACTIVE MAGNETIC bearings (AMBs) comprise a number of electromagnets which are actively controlled to support a ferromagnetic rotor using position feedback. They have several advantages over conventional bearings. In particular, their contactless nature facilitates very high-speed rotation and operation over wide temperature and pressure ranges. They are, therefore, being employed in an ever-increasing range of applications. During the last two decades, numerous investigations related to the control aspects of AMBs have been reported, eg., [1] and [2]. Regarding models of magnetic bearings, there are essentially two basic forms: 1) voltage control, which is suitable for sensorless operation, and for which various control strategies based on observers have been reported [3], [4] and 2) current-control, which is appropriate when position sensors are employed. The order of the model is then lower and, hence, the bearing is easier to control and, in many cases, the active bearing can be modeled as a second-order system, but subject to both parameter uncertainties and disturbances. In theory, classical proportional–derivative (PD) or proportional–integral–derivative (PID) controllers can provide stability, although they require velocity feedback, either from direct sensor input or differentiation of position data. However, this is often problematic due to system noise and the small rotor displacement range.

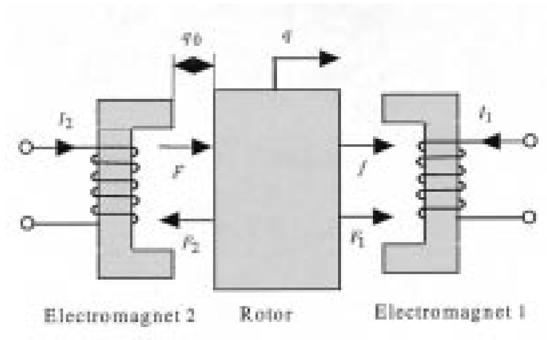

Fig. 1. Basic magnetic bearing.

This paper considers a basic AMB system comprising an electromagnet on each side of a rigid rotor, as shown in Fig. 1. The model on which the controller design is based is described by a second-order linear interval system with unknown disturbances. The parameter uncertainty in the system is well described by the given parameter intervals, while the unmodeled dynamics may be included in the disturbance. To eliminate the need for velocity feedback, a dynamical compensator is proposed which uses only the rotor position signal. In designing the controller, three closed-loop specifications are addressed: robust stabilization, disturbance attenuation, and minimum control effort. By deriving stability conditions for the closed-loop system, a characterization of all the robust stabilizing dynamical compensators for the interval system is obtained. This characterization is in terms of four design parameters representing the degrees of freedom in the controller. It is readily shown that the disturbances in the AMB system cannot be decoupled from the position (output) signal. In order to attenuate the effect of disturbances to the position output of the system, the H_2 norm of the transfer function from the disturbance to the position output is minimized over the system parameter intervals, by optimizing the design parameters in the robust stabilizing controller. Three sets of dynamical compensators are derived, all of which robustly stabilize the interval system, while, at the same time, providing the desired H_2 norm of the transfer function from the disturbance to the system position output. Minimum effort

Paper IPCSD 00–041, presented at the 1999 IEEE International Electric Machines and Drives Conference, Seattle, WA, May 9–12, and approved for publication in the IEEE TRANSACTIONS ON INDUSTRY APPLICATIONS by the Industrial Drives Committee of the IEEE Industry Applications Society. Manuscript submitted for review July 2, 1999 and released for publication July 24, 2000. This work was supported by the European Commission under the BRITE-EURAM Programme and by the Chinese National Outstanding Youth Science Foundation under Grant 69504002.

G. R. Duan is with the School of Mechanical and Manufacturing Engineering, The Queen's University of Belfast, Belfast, BT9 5AH, U.K., on leave from the Research Office for Control Systems Theory, Harbin Institute of Technology, Harbin 150001, China (e-mail: G.R.Duan@qub.ac.uk).

Z.-Y. Wu, C. Bingham, and D. Howe are with the Electrical Machines and Drives Group, Department of Electronic and Electrical Engineering, University of Sheffield, Sheffield S1 3JD, U.K. (e-mail: w.zahn-yuan@sheffield.ac.uk; c.bingham@sheffield.ac.uk; d.howe@sheffield.ac.uk).

Publisher Item Identifier S 0093-9994(00)10422-0.

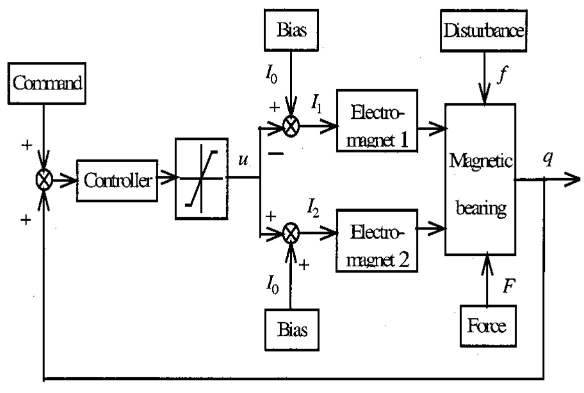

Fig. 2. Diagram of the control system.

control provides the advantages of reducing input energy, and minimizing the likelihood of control saturation. However, since practical magnetic bearing systems contain nonlinearities, and the controller design is based only on a linearized model, the control system is guaranteed to be stable only if it operates close to its equilibrium position. This means that the input and output variables of the system must be kept close to zero. By using the free parameter(s) in the set of controllers which robustly stabilize the interval system and meet the disturbance attenuation requirement, dynamical compensators are obtained which also keep the control effort close to a minimum bound to an arbitrary degree.

II. Problem Formulation

A dynamical mathematical model for the AMB shown in Fig. 1, can be established as follows:

$$m\ddot{q} = -\frac{\mu_0 AN^2}{4}\left[\left(\frac{I_1}{q_0 - q}\right)^2 - \left(\frac{I_2}{q_0 + q}\right)^2\right] + f + F \quad (1)$$

where

m	mass of the rotor (kg);
q	position displacement of the rotor (m);
q_0	nominal air gap (m);
μ_0	permeability of free space $= 4\pi \times 10^{-7}$ H/m;
A	total pole-face area of each electromagnet (m^2);
N	number of turns on each electromagnet coil;
I_1, I_2	electromagnet coil currents (A);
f	an unknown disturbance (N);
F	some known force acting on the rotor (N).

When (1) is linearized at the equilibrium point, ie.,

$$I_1 = I_2 = I_0 \quad q = 0$$

and augmented with the control structure shown in Fig. 2, the linearized model is obtained as the following second-order system:

$$\ddot{q} - \omega^2 q = \sigma u + \frac{1}{m}(f + F) \tag{2a}$$

where

$$\omega^2 = \frac{\mu_0 AN^2 I_0^2}{mq_0^3} \quad \sigma = -\frac{\mu_0 AN^2 I_0}{mq_0^2}. \tag{2b}$$

Due to inaccuracies in the measurement of some of the physical parameters and changing environmental conditions, the system parameters ω and σ are generally uncertain. However, without loss of generality, it can be assumed that their values lie within some known intervals

$$\omega \in [\omega_1 \quad \omega_2] \quad \sigma \in [\sigma_1 \quad \sigma_2]$$

where ω_1, ω_2, σ_1, and σ_2 are known scalars satisfying

$$\omega_2 \geq \omega_1 > 0 \quad \sigma_1 \leq \sigma_2 < 0.$$

It is clear that, in order to stabilize the system (2), either a PD or a PID controller is adequate. When such controllers are used, however, the differential component has to be present in order to achieve closed-loop stability, since the open-loop system (2) is unstable. In order to avoid the need for velocity feedback, while at the same time achieving satisfactory stability, this paper addresses the control of the system (2) using a dynamical position feedback compensator.

Assuming that only the rotor displacement position q is measured, and denoting

$$x = \begin{bmatrix} q \\ \dot{q} \end{bmatrix} \quad y = q$$

the system (2) can be converted into the following equivalent state-space form:

$$\begin{cases} \dot{x} = A_m x + b_m u + d_m(f + F) \\ y = c_m x \end{cases} \tag{3a}$$

with

$$A_m = \begin{bmatrix} 0 & 1 \\ \omega^2 & 0 \end{bmatrix}$$
$$b_m = \begin{bmatrix} 0 \\ \sigma \end{bmatrix}$$
$$d_m = \begin{bmatrix} 0 \\ 1/m \end{bmatrix}$$
$$c_m = [1 \quad 0] \tag{3b}$$

where the parameters ω and σ satisfy

$$\omega_2 \geq \omega \geq \omega_1 > 0 \quad \sigma_1 \leq \sigma \leq \sigma_2 < 0. \tag{4}$$

Thus, the system (3) is still an interval system, but is now in state-space form. A general first-order output dynamical compensator for the system (3) can be written in the following form [5]:

$$\begin{cases} \dot{z} = k_{22} z + k_{21} y \\ u = k_{11} y + k_{12} z + k_f F \end{cases} \tag{5}$$

where k_{ij}, $i, j = 1, 2$, are four scalar controller coefficients, to be designed, and the term $k_f F$ is introduced to compensate for the effect of the force F, the coefficient k_f being given by

$$k_f = -\frac{1}{m\sigma} = \frac{q_0^2}{\mu_0 A N^2 I_0}.$$

Denoting $\xi^T = [x\ z]$, and applying the dynamical compensator (5) to the system (3), results in the closed-loop state-space description

$$\begin{cases} \dot{\xi} = A_{mc}\xi + d_{mc} f \\ y = c_{mc}\xi \end{cases} \tag{6a}$$

with

$$\begin{aligned} A_{mc} &= \begin{bmatrix} A_m + b_m k_{11} c_m & b_m k_{12} \\ k_{21} c_m & k_{22} \end{bmatrix} \\ &= \begin{bmatrix} 0 & 1 & 0 \\ \sigma k_{11} + \omega^2 & 0 & \sigma k_{12} \\ k_{21} & 0 & k_{22} \end{bmatrix} \end{aligned} \tag{6b}$$

$$\begin{aligned} c_{mc} &= [1 \quad 0 \quad 0] \\ d_{mc}^T &= \begin{bmatrix} 0 & \dfrac{1}{m} & 0 \end{bmatrix} \end{aligned} \tag{6c}$$

where the parameters ω and σ satisfy (4).

This paper considers the design of a dynamical compensator of the form (5) to meet three requirements: robust stabilization, disturbance attenuation, and minimum control effort, for the closed-loop system (6).

III. Controller Design

A. Robust Stabilization

Through direct analysis of the stability of the matrix A_{mc} in (6b), all the robust stabilizing compensators in the form of (5) for the system (3) can be characterized by the following:

$$\begin{cases} k_{11} = -\dfrac{1}{\sigma}(\omega^2 + \alpha) \\ k_{12} = \gamma \\ k_{22} = -\beta \\ k_{21} = \dfrac{\alpha\beta\tau}{\sigma\gamma} \end{cases} \tag{7}$$

where α, β, γ and τ are real scalars satisfying

$$\alpha > 0 \quad \beta > 0 \quad \gamma \neq 0, \qquad 0 < \tau < 1. \tag{8}$$

B. Disturbance Attenuation

When the system (3) is robustly stabilized with the dynamical compensator (5), the closed-loop system (6) maintains stability over the whole parameter interval range. However, due to the effect of the unknown disturbance f, the performance of the closed-loop system may be poor. To overcome this, it is preferable to have the effect of the disturbance f completely decoupled from the system output through control. However, this can easily be shown to be unfeasible for this AMB system. Note that the contribution of the disturbance f to the output y is given, in the frequency domain, by

$$y(s) = c_{mc}(sI - A_{mc})^{-1} d_{mc} f(s). \tag{9}$$

In order to attenuate the effect of the disturbance, it is appropriate to minimize

$$N = \left\| c_{mc}(sI - A_{mc})^{-1} d_{mc} \right\|_2^2. \tag{10}$$

This can be realized directly if the system parameters are accurately known. However, since the system (3) is an interval system, the index N in (10) is not unique. To overcome this difficulty, instead of minimizing the index N, the following may be minimized:

$$N' = \sup_{\substack{\omega \in [\omega_1\ \omega_2] \\ \sigma \in [\sigma_1\ \sigma_2]}} \left\| c_{mc}(sI - A_{mc})^{-1} d_{mc} \right\|_2^2 \tag{11}$$

where the index N' accounts for the worst case obtained from the parameter interval ranges. Thus, the disturbance attenuation problem can be described as finding the dynamical compensators in the form of (5), which robustly stabilize the interval system (3) and, simultaneously, guarantee that $N' \leq \varepsilon_0$, where ε_0 is an arbitrarily small positive scalar.

When the robustly stabilizing dynamical compensator given in (7) is applied to the interval system (3) N' is given by

$$N' = \frac{1}{2\alpha\beta\tau} + \frac{\beta}{2\alpha^2\tau(1-\tau)}. \tag{12}$$

The robust stabilizing dynamical compensator for the interval system (3) given by (7)

1) guarantees the disturbance attentuation specification in (11) if

$$\alpha = \frac{1 + \sqrt{1 + 8\varepsilon_0\beta^3 \dfrac{\tau}{1-\tau}}}{4\varepsilon_0\beta\tau} \tag{13}$$

2) and minimizes N' with respect to β, if

$$\begin{cases} \alpha = \dfrac{1}{\sqrt[3]{\varepsilon_0^2\tau^2(1-\tau)}} + \theta^2 \\ \beta = \sqrt{\left(\dfrac{1-\tau}{\varepsilon_0\tau}\right)^{2/3} + \theta^2(1-\tau)} \end{cases} \tag{14}$$

3) and minimizes N' with respect to both β and τ, if α, β and τ are taken as

$$\begin{cases} \alpha = 3\left(\dfrac{1}{\sqrt[3]{2\varepsilon}} + \theta^2\right)^2 \\ \beta = \dfrac{1}{\sqrt[3]{2\varepsilon}} + \theta^2 \\ \tau = \dfrac{2}{3} \end{cases} \tag{15}$$

where θ is an arbitrary real scalar.

C. Minimum Control Effort

The controller given in (5) can be written, in the frequency domain, as

$$u(s) = G_{uy}(s)y(s) \tag{16a}$$

with

$$G_{uy}(s) = \left(\frac{k_{12}k_{21}}{s - k_{22}} + k_{11}\right). \tag{16b}$$

In order to facilitate small control effort, the following index is proposed for minimization:

$$J = \left\|\frac{k_{12}k_{21}}{s - k_{22}} + k_{11}\right\|_\infty \tag{17}$$

which can be shown to have the greatest lower bound

$$J_{glb} = \frac{\omega_2^2}{|\sigma_2|}. \tag{18}$$

Therefore, the control effort specification can be written, more specifically, as follows:

$$J - \frac{\omega_2^2}{|\sigma_2|} = \left\|\frac{k_{12}k_{21}}{s - k_{22}} + k_{11}\right\|_\infty - \frac{\omega_2^2}{|\sigma_2|} \le \varepsilon_u \tag{19}$$

where ε_u is an arbitrarily given positive scalar.

The robust dynamical stabilizing compensator given by (7) for the interval system (3) guarantees the disturbance attenuation specification in (11) and

1) meets the control effort restriction (19), if α is taken as in (13) and

$$\tau = \frac{\beta^2 + |\sigma_2|\varepsilon_u}{\beta^2 + |\sigma_2|\varepsilon_u\,(1 + 2|\sigma_2|\beta\varepsilon_0\varepsilon_u)} \tag{20}$$

where β is a nonzero positive scalar

2) meets the control effort restriction (19), and minimizes the index N' with respect to β, if

$$\begin{cases} \alpha = \dfrac{1 + \varepsilon_0\sqrt{(\varepsilon_u|\sigma_2|)^3}}{\varepsilon_0\sqrt{\varepsilon_u|\sigma_2|}} \\ \beta = \sqrt{\varepsilon_u|\sigma_2|} \\ \tau = \dfrac{1}{1 + \varepsilon_0\sqrt{(\varepsilon_u|\sigma_2|)^3}}. \end{cases} \tag{21}$$

IV. Simulation and Experimental Results

This section deals with the application of the preceding robust stabilizing controller design procedure to the active magnetic bearings of a flywheel energy storage system.

A. Flywheel Energy Storage Unit

The active magnetic bearings are integral components of a flywheel energy storage system which is being developed as a peak power buffer for urban electric vehicles [6]. The flywheel is a carbon–fiber composite rim, which is supported by two active radial magnetic bearings and two passive axial magnetic bearings, and contained within an evacuated enclosure, as shown schematically in Fig. 3. A permanent-magnet (PM) brushless machine is incorporated within the flywheel to transform kinetic energy to electrical energy, and vice-versa. The flywheel is designed to rotate at a maximum speed of 60 000 r/min, and provides a recoverable energy of 350 Wh in slowing down to half speed, the peak power capability being 40 kW. The magnetic bearing system has been designed to cope with the dominant disturbances which result from gyroscopic effects arising from the motion of the vehicle, and the high-frequency forces due to unbalance of the rim.

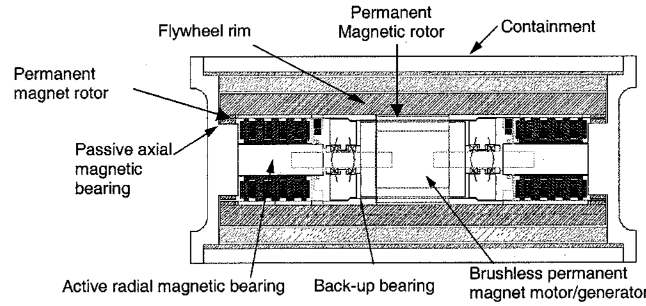

Fig. 3. Schematic of flywheel energy storage unit.

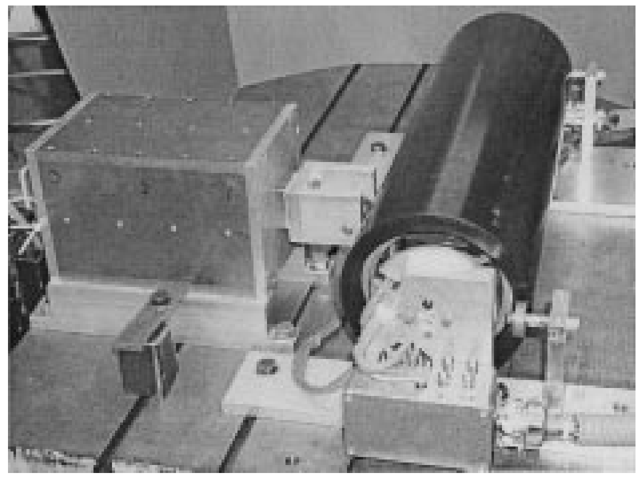

Fig. 4. Demonstrator flywheel rim and controllable force actuator.

The rim of the flywheel unit, together with a short-stroke actuator by which a controlled disturbance force can be applied, is shown in Fig. 4.

The active radial bearings have a homopolar magnetic circuit topology and a soft magnetic composite rotor, in order to minimize hysteresis and eddy-current losses in the rotor. The active pole-face area of the electromagnets on the vertical axes is twice that of the electromagnets on the horizontal axes, the respective peak force capabilities being 1600 and 800 N, respectively.

An eddy-current rotor displacement sensor, with a resolution of 1 μm, a linearity of 1% of full scale, and a frequency bandwidth of 5 kHz, is used on each axis for closed-loop control. The coil of each electromagnet is supplied from a current-controlled switched-mode power amplifier, with appropriate features to reduce noise. The total mass of the rim is 12 kg. The nominal parameters for the bearings are given in Table I.

TABLE I
BEARING PARAMETERS

Parameter	Vertical axis	Horizontal axis
m	6 kg	6 kg
A	$4\times2.6\times10^{-4}$ m^2	$4\times1.3\times10^{-4}$ m^2
N	40	40
I_0	5 A	5 A
q_0	0.4 mm	0.4 mm

TABLE II
PARAMETERS ω AND σ, AND THEIR LOWER AND UPPER BOUNDS

Parameter	Vertical	Horizontal
ω	359.6	254.3
σ	-10.35	-5.17
ω_1	240	170
ω_2	390	280
σ_1	-22	-10
σ_2	-4.5	-2

Since

$$I_1 = I_0 + u, \quad I_2 = I_0 - u$$

the coil currents must be controlled to ensure $|u| \le I_0$.

B. Nonlinear Simulation

When the dynamical compensator (5) is applied to the original nonlinear system (1), with a consideration of current saturation as in Fig. 2, the closed-loop system is

$$\begin{cases} \dot{q} = q' \\ \dot{q}' = \dfrac{\mu_0 A N^2}{4m}\left[\left(\dfrac{I_0-u}{q_0-q}\right)^2 - \left(\dfrac{I_0+u}{q_0+q}\right)^2\right] + \dfrac{1}{m}(F+f_d) \\ \dot{z} = k_{21}q + k_{22}z \\ u = \begin{cases} I_0, & \text{if } k_{11}y+k_{12}z+k_fF > I_0 \\ k_{11}y+k_{12}z+k_fF, & \text{if } |k_{11}y+k_{12}z+k_fF| \le I_0 \\ -I_0, & \text{if } k_{11}y+k_{12}z+k_fF < -I_0 \end{cases} \\ y = q. \end{cases}$$

In order to simulate the system, the parameters ω and σ and their upper and lower bounds are determined from (2b), based on the parameter values in Table I. In order that the designed controller can tolerate sufficient parameter uncertainties, large intervals for ω and σ were chosen. The values of ω and σ, and those of the interval boundaries, ω_i and σ_i, $i = 1, 2$, for both the vertical and horizontal axes, are given in Table II. Choosing $\varepsilon_0 = 10^{-10}$, $\varepsilon_u = 1$, $\beta = 5 \times 10^3$, and $\gamma = 10^4$, the coefficients of the dynamical compensators are obtained as shown in Table III.

TABLE III
CONTROLLER COEFFICIENTS

Coefficients	Vertical	Horizontal
k_{11}	256x10^4	5392x10^3
k_{12}	10^4	10^4
k_{21}	-111x10^3	-250x10^3
k_{22}	-5x10^3	-5x10^3
k_f	0.0161	0.0161

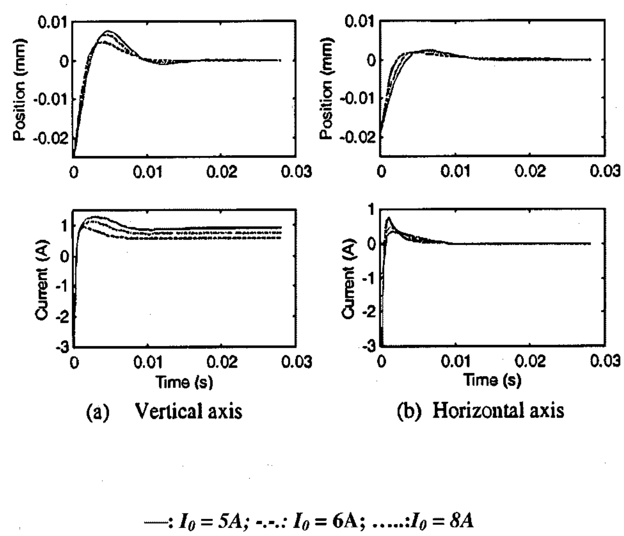

Fig. 5. Initial excitation of single bearing (—: $I_0 = 5$ A; $-\cdot-\cdot$: $I_0 = 6$ A; $\cdots$: $I_0 = 8$ A).

In the nonlinear closed-loop simulation, the active force F was assumed to be 6 × 9.8 N for the vertical axis of each of the bearings, and zero for the horizontal axis. The responses of the x and y axes when one of the bearings is initially excited, with a bias current $I_0 = 5$ A, with the controller coefficients specified in Table III, is shown in Fig. 5. A change of I_0 results in changes to the parameters ω and σ and, hence, affects the performance, and may even compromise the stability of the control system. In order to illustrate the robustness of the designed control system with respect to parameter perturbations, simulation responses with $I_0 = 6$ A and 8 A, are also included in Fig. 5. While the change of I_0 has clearly affected the transient characteristics, the results demonstrate that a degree of stability (and performance) robustness has been imparted to the system under the influence of parameter variations.

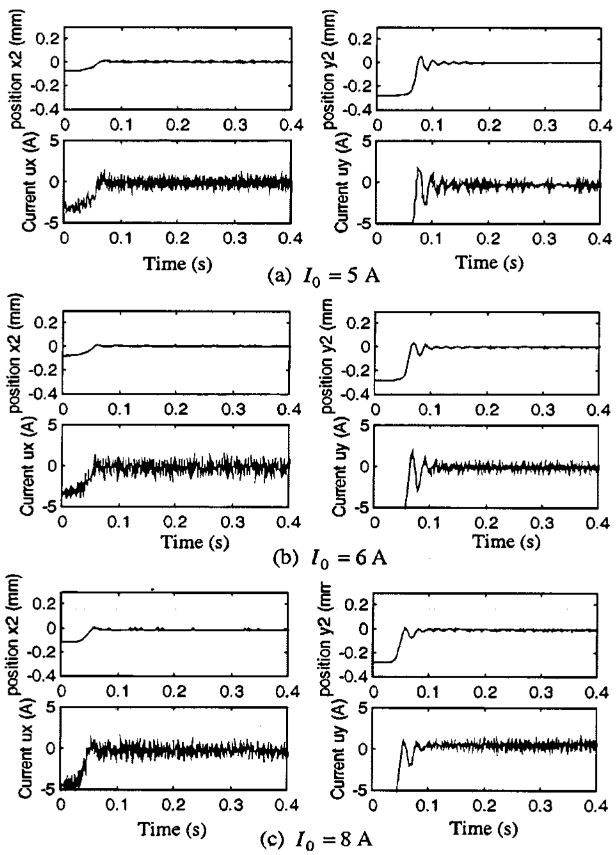

Fig. 6. Initial excitation of single bearing.

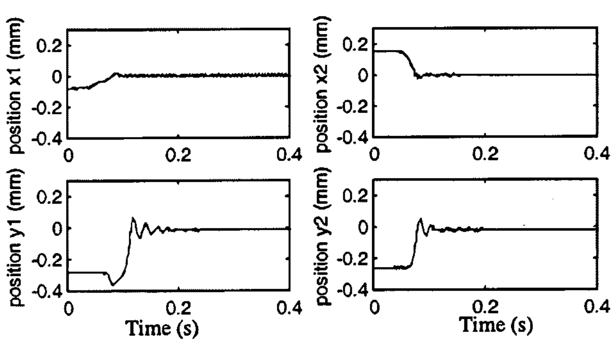

Fig. 7. Initial excitation of bearing system ($I_0 = 5$ A).

C. Experimental Results

Digital implementation of the control structure (with parameters as in Table III) was carried out using a TMS320C40/DSPACE hardware development platform. The sampling rate for controller implementation was 10 kHz.

In order to experimentally validate the stability robustness and performance predictions, the transient excitation response of one bearing "x_2, y_2" was measured. Fig. 6 shows the resultant dynamics for $I_0 = 5$, 6, and 8 A. It can be seen that a degree of stability robustness has been obtained, and the performance varies only marginally with a change of I_0. Figs. 5 and 6 demonstrate the usefulness of the interval system approach to control system design, since, although the nonlinear model used for the simulation studies has not encompassed all the dynamic modes of the flywheel, as exemplified by the relatively underdamped characteristics of the actual transient response, the interval method for robust controller design has addressed the problem of model uncertainty, and demonstrated satisfactory stability and performance attributes.

As a consequence of manufacturing tolerances, the dynamic characteristics of the magnetic bearings at the two ends of the flywheel will differ. However, the interval approach to controller design is sufficiently robust that the same control structure can be applied to each bearing. Fig. 7 shows the transient response following initial excitation of all bearings. As predicted, the system exhibits satisfactory dynamic characteristics, the maximum overshoot being ≈0.04 mm.

In addition to the controller designs given in Table III, others have been simulated and experimentally assessed. For example, different controllers have been employed for the vertical and horizontal axes electromagnets at each end of the flywheel, to account for variations in their performance parameters, and this has yielded improved performance. However, in order to demonstrate the robustness issues pertinent to interval systems, this paper has only considered the performance when the same controller is used for both axes.

V. Conclusions

This paper has addressed the robust stabilization of AMBs to support a high-speed energy storage flywheel. It has considered the design of dynamical compensators to provide robust stabilization, disturbance attenuation, and minimum control effort. Throughout, it has assumed that an accurate model of the AMB, encompassing all the dominant dynamic modes, is unavailable for controller design. Interval system analysis has been used to design appropriate controllers, and thereby overcome the detrimental effects of modeling uncertainty. Simulation studies have illustrated the predicted stability and performance robustness properties, whilst, the digital implementation has enabled the practical attributes of dynamic compensator design without the need for direct velocity feedback, to be assessed.

References

[1] R. Stanway and J. O'Reilly, "State variable feedback control of rotor bearing suspension systems," in *Proc. 3rd Int. Conf. Vibrations in Rotating Machinery*, 1984, pp. C277–C284.

[2] J. Y. Hung, " Magnetic bearing control using fuzzy logic," *IEEE Trans. Ind. Applicat.*, vol. 31, pp. 1492–1497, Nov./Dec. 1995.

[3] H. Bleuler, D. Vischer, G. Schweitzer, A. Traxler, and D. Zlatnik, "New concepts for cost-effective magnetic bearing control," *Automatica*, vol. 30, no. 5, pp. 871–876, 1994.

[4] T. Mizuno, K. Araki, and H. Bleuler, "Stability analysis of self-sensing magnetic bearing controllers," *IEEE Trans. Contr. Syst. Technol.*, vol. 4, pp. 572–579, Sept. 1996.

[5] G. R. Duan, "Robust eigenstructure assignment via dynamical compensators," *Automatica*, vol. 29, no. 2, pp. 469–474, 1993.

[6] P. Mason, K. Atalla, Z. Y. Wu, D. Howe, and P. H. Mellor, "A flywheel peak power buffer for electric vehicles," in *Proc. EVS15*, 1998, pp. 379–388.

Guang-Ren Duan (M'91–SM'95) received the B.Sc. degree in applied mathematics and the M.Sc. and Ph.D. degrees in control engineering from Harbin Institute of Technology, Harbin, China.

From 1989 to 1991, he was engaged in post-doctoral work at Harbin Institute of Technology, where, since 1992, he has been a Professor of Control Systems Theory. He has visited a number of universities in the U.K. and is currently on leave at The Queen's University of Belfast, Belfast, U.K. His main research interests include robust control, eigenstructure assignment, descriptor systems, missile autopilot design, and magnetic bearing control.

Dr. Duan is a Chartered Engineer in the U.K. and a Fellow of the Institution of Electrical Engineers, U.K.

Zhan-Yuan Wu received the B.Eng. and M.Sc. degrees in control engineering from Northeastern University, Shenyang, China, and the Ph.D. degree from the University of Sheffield, Sheffield, U.K., in 1985, 1988, and 1999, respectively.

From 1988 to 1991, he was an Assistant Lecturer in the Department of Automatic Control, Northeastern University. He is currently a Research Associate at the University of Sheffield. His research interests include novel power electronic drive topologies and control of active magnetic bearings.

Chris Bingham (M'00) received the B.Eng. degree in electronic systems and control engineering from Sheffield City Polytechnic, Sheffield, U.K., the M.Sc.(Eng.) degree in control systems engineering from the University of Sheffield, Sheffield, U.K., and the Ph.D. degree from Cranfield University, Cranfield, U.K., in 1989, 1990, and 1994, respectively.

He was a Post-Doctoral Researcher at Cranfield University until taking up a research position at the University of Sheffield, where, since 1998, he has been a Lecturer in the Department of Electronic and Electrical Engineering.

David Howe received the B.Tech. and M.Sc. degrees from the University of Bradford, Bradford, U.K., and the Ph.D. degree from the University of Southampton, Southampton, U.K., in 1966, 1967, and 1974, respectively, all in power engineering.

He has held academic posts at Brunel and Southampton Universities, and spent a period in industry with NEI Parsons Ltd., working on electromagnetic problems related to turbogenerators. He is currently Lucas Professor of Electrical Engineering at the University of Sheffield, Sheffield, U.K., where he heads the Electrical Machines and Drives Research Group. His research activities span all facets of controlled electrical drive systems, with particular emphasis on permanent-magnet excited machines. He is the author of approximately 300 publications in the fields of machines, drives, and motion control systems.

Prof. Howe is a Chartered Engineer in the U.K. and a Fellow of the Institution of Electrical Engineers, U.K.